Deterministic Microgrinding, Lapping, and Polishing of Glass-Ceramics

Introduction

Glass-ceramics are attractive structural materials due to their good mechanical properties, chemical stability at higher temperatures, and tailored microstructures via appropriate heat treatments. In the cold working of glass-ceramics, several options are available: loose-abrasive grinding (lapping, at fixed nominal pressure) or deterministic microgrinding (at fixed nominal infeed, with bound-abrasive tools), both of which primarily remove material by microcracking. These manufacturing operations are usually followed by polishing to remove the residual stresses or damage left from the grinding operations.

The goal of the work described in this article is twofold: to determine which properties of glass-ceramics are responsible for material removal and the quality of the resulting surface (roughness, residual stresses induced by grinding), and to compare loose-abrasive grinding with deterministic microgrinding.

Measurements

Five novel glass-ceramic materials (labeled GC1-GC5) were provided by Corning, Inc. The surface roughness of the as-received samples was in the range of 4 to 8 μm (peak-to-valley).

1. Elastic Properties and Microindentation Measurements

Longitudinal and shear wave speeds were first measured and then converted to Young's and shear moduli. Young's modulus was also independently measured from the load-displacement curve in 4-pt bending tests. Modulus of rupture was measured in 4-pt bend tests for as-received samples, as well as for samples in which controlled flaws were introduced on the tension side by Vickers indentation. Knoop hardness was measured at loads of 50 to 200 gf. Vickers hardness was measured at loads from 10 to 1000 gf. Between five to ten indents at each load were performed (15-s dwell time). All materials were measured in air.

For the fracture toughness measurements, the length c of the cracks emanating from the Vickers indentation corners was measured optically. We used indentation[1]—the approach of Evans[2]—to extract the fracture toughness K_c from the measured indentation crack size. In our glass-ceramics tests, the range of indentation crack size to indent diagonal $c/(D/2)$ was from 2 to 3 and thus covered by the Evans approach. Ponton and Rawlings[3,4] published an exhaustive analysis comparing the prediction of the fracture toughness by many different indentation models to the fracture toughness measured by bulk methods. They examined many ceramics (zirconias and aluminas), as well as many glass-ceramics, concluding that several models gave good agreement between the bulk and indentation fracture toughness measurements. The Evans model[2] was one such model. Our work on the fracture toughness of optical glasses[5] also has shown that the Evans model provides a good prediction of fracture toughness.

2. Chemical Susceptibility Measurements

The alkali resistance of the glass-ceramics was tested by immersing two test pieces in a boiling aqueous solution of equal parts Na_2CO_3 and $NaOH$ for 3 h. The resulting mass loss, measured in an analytical balance, indicates the material's chemical susceptibility or alkali resistance. Table 97.II summarizes the measured micromechanical and chemical properties of the glass-ceramic materials.

3. Deterministic Microgrinding Measurements

Deterministic microgrinding is a fixed-infeed-rate material removal process utilizing computer-numerically-controlled (CNC) machining platforms. We sequentially used three thin-walled diamond-bound-abrasive (metal bond 75N, medium hardness) cup wheel tools on the Opticam SX CNC machining platform.[6] The tools were dressed before grinding each new type of material. To examine the effect of abrasive size in deterministic microgrinding, we used the three tools on glass-ceramics samples in the form of thin disks (aspect ratio about 30/1): first, a rough tool (average abrasive size of 70 μm) at an infeed rate of 100 μm/min, then a medium tool (abrasive size 10 to 20 μm) at an infeed rate of 50 μm/min, and finally a fine tool (abrasive size 2 to 4 μm) at an infeed rate of 10 μm/min. The tool rotation rate was 5000 rpm, and the work rotation rate

was 150 rpm. The tool rotation rate and diameter correspond to a surface speed of about 14.1 m/s. Three to five samples were tested at each setting. Following grinding with each tool, the surface roughness was measured with a white-light interferometer (Model NewView 1000, Zygo Corp., Middlefield, CT) and so was the power (sag), induced by the grinding process.

4. Loose-Abrasive Lapping and Polishing
   Removal Rate Measurements
   Lapping and polishing experiments used thin glass-ceramic disks of approximately 2.2-mm thickness and 62-mm diameter. The as-received saw-cut specimens were first lapped on a Strasbaugh platform with 22-μm alumina abrasives (cast-iron plate and aqueous slurry), then with 7-μm alumina abrasives (same slurry composition), and finally polished with 1-μm alumina abrasives (aqueous slurry, new polyurethane lap used for each material). The initial condition for each process was the final surface from the previous step. In the

lapping and polishing experiments, the pressure was maintained at 10 to 14 kPa and the relative speed at 1.22 m/s. Surface roughness was measured at the center and near the edge of the circular surfaces.

5. Grinding-Induced Surface Residual Stress Measurements
   Surface residual stresses induced by the lapping process (see the previous section), i.e., the Twyman effect for glass-ceramics, were measured on flat disks of samples (aspect ratio of about 30/1) whose two sides (S1 and S2) were first polished to approximately one-wave flatness. Subsequently, one surface (surface S1) was lapped by 22-μm Al_2O_3 abrasives for about 2 to 3 min, then by 7-μm Al_2O_3 abrasives for about 30 min, and finally polished by 1-μm Al_2O_3 abrasives for about 20 to 45 min. The slurry and processing conditions were as described in the previous section. During this process, the other surface (S2) remained polished, and its power (sag) was measured with the white-light interferometer.

Table 97.II: Summary of the measurements of the mechanical and chemical properties of glass-ceramics.

	GC1	GC2	GC3	GC4	GC5
Thermoelastic properties					
Density ρ (kg m^{-3})	3.18	2.93	2.98	2.99	2.98
Thermal expansion coefficient α (10^{-6} °C^{-1})	8.6	6.02	–	–	4.21
Young's modulus E (GPa), ±5%	130	130	123	138	113
Shear modulus G (GPa), ±5%	52.2	53.4	48.9	56.8	46.0
Poisson ratio ν	0.242	0.219	0.255	0.217	0.229
Modulus of rupture (MPa), ±10%					
As-received	178	162	145	159	124
With Vickers flaw @ P = 1 kgf	138	120	80	118	76
Microindentation hardness					
Knoop hardness @ 0.2 kgf (GPa), ±5%	9.3	10.0	9.4	9.9	8.7
Vickers hardness @1 kgf (GPa), ±10%	9.5	9.4	9.3	10.0	8.2
Microindentation cracking					
Crack size $2c$ (μm) @ 500 gf	83.6	70.6	81.7	73.0	80.8
Indent. fracture toughness K_c $\left(MPa \sqrt{m}\right)$, ±10%	1.41	1.75	1.53	1.63	1.55
Chemical susceptibility (alkali attack)					
Mass loss per unit area (mg/cm^2)	162±20	43±12	41.3±3.3	33±2.3	114±0.3

Results

For the deterministic microgrinding experiments (fixed infeed rate), Fig. 97.44 shows the correlation of surface roughness and chemical susceptibility (alkali resistance). The results generally indicate that materials with higher chemical susceptibility also lead to higher surface roughness. Figure 97.45 shows the correlation of surface microroughness with abrasive size, indicating that, for a given material, finer abrasives lead to lower surface roughness. Figure 97.46 shows the dependence of the grinding-induced surface residual force per unit length on the Vickers indentation crack size.

For the loose-abrasive lapping experiments, Fig. 97.47 shows the dependence of the material removal rate on the material figure of merit $E^{5/4}/[K_c \, Hv]$, Fig. 97.48 the dependence of surface microroughness on hardness, and Fig. 97.49 the dependence of surface roughness on chemical susceptibility.

For the polishing experiments, Fig. 97.50 shows the dependence of the polishing rate on Vickers hardness and Fig. 97.51 the polishing rate versus the material figure of merit $E^{5/4}/[K_c \, Hv]$. Figure 97.52 shows the dependence of the lapping-induced surface-grinding force on microindentation crack size.
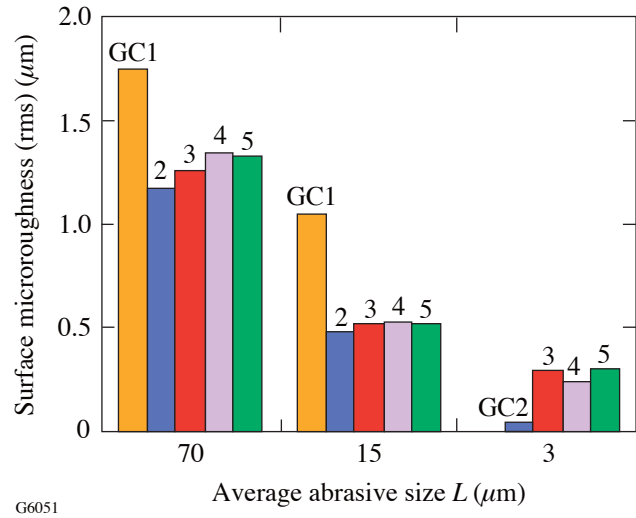

G6051

Figure 97.45
Dependence of surface microroughness on abrasive size in deterministic microgrinding.
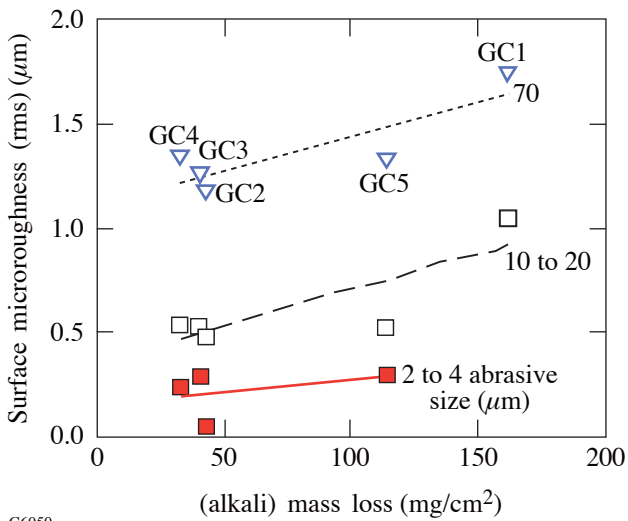

G6050

Figure 97.44
Dependence of surface roughness induced by deterministic microgrinding on chemical susceptibility, as measured by the mass loss under alkali attack.
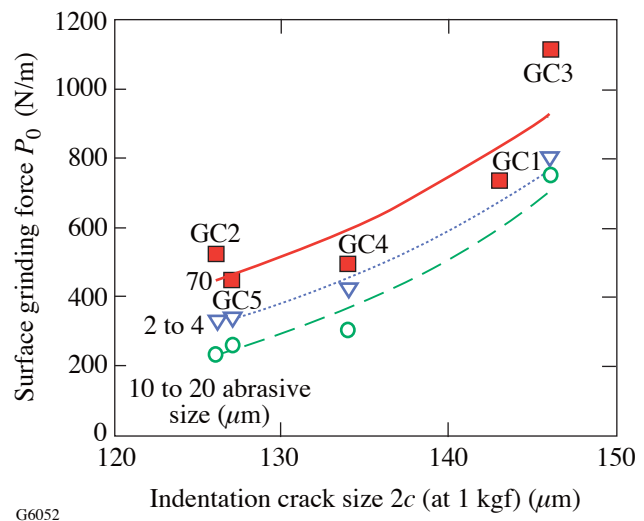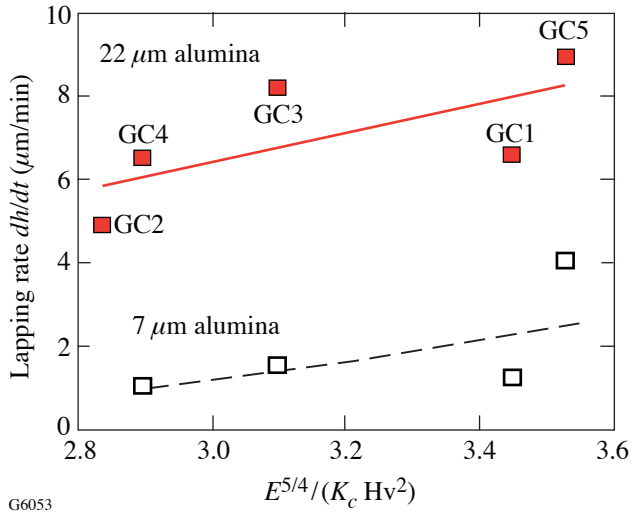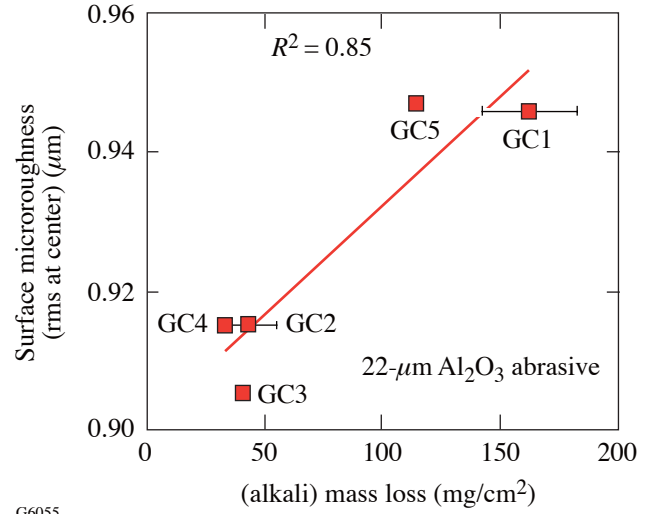

G6052

Figure 97.46
Dependence of grinding-induced force P_0 on indentation crack size (at 1 kgf).
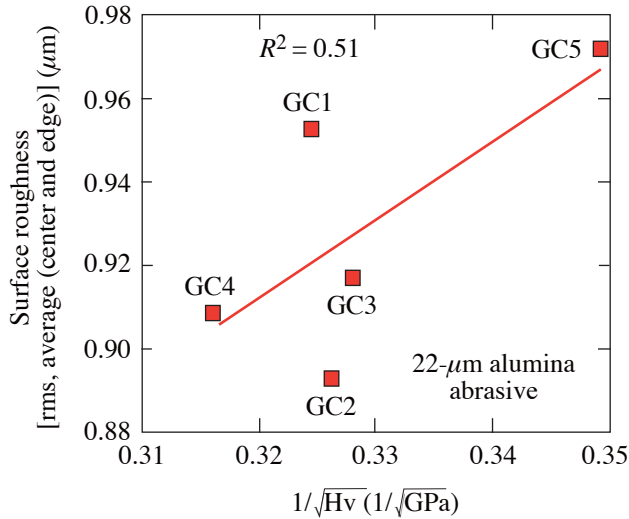
G6053

Figure 97.47
Dependence of lapping rate on mechanical properties. Fracture toughness K_c (MPa m$^{1/2}$) and Vickers hardness Hv (GPa, at 1 kgf).
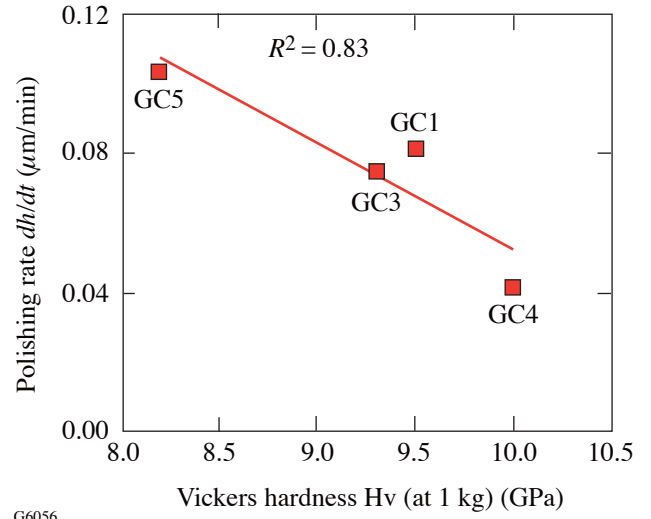

G6055

Figure 97.49
Dependence on chemical susceptibility of surface roughness (measured in center of the plate) induced by lapping with 22-μm Al$_2$O$_3$ abrasives.

G6054

Figure 97.48
Dependence of surface roughness induced by lapping with 22 μm Al$_2$O$_3$ on material hardness.

G6056

Figure 97.50
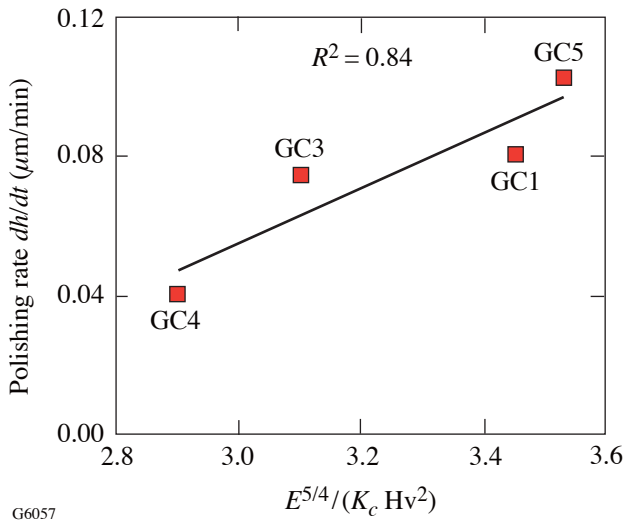Dependence of polishing rate on Vickers hardness (at 1 kgf).

G6057

Figure 97.51

Dependence of polishing rate on mechanical properties: fracture toughness K_c (MPa m$^{1/2}$) and Vickers hardness Hv (GPa, at 1 kgf) from microindentation.
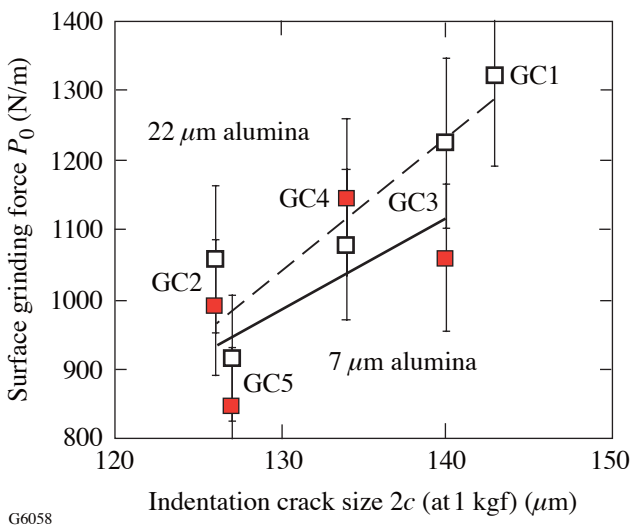

G6058

Figure 97.52

Dependence on microindentation crack size (at 1 kgf) of lapping-induced surface grinding force P_0 for lapping with 22-μm and 7-μm Al$_2$O$_3$ abrasives. The lapped surface is S1 (originally polished). P_0 is proportional to the change in power, measured on the polished surface S2, from the initial power (S1 polished) to the value after S1 is lapped.

Discussion

Some of our results are as intuitively expected. For example, Figs. 97.44 and 97.49 indicate that higher chemical susceptibility leads to higher surface roughness, both under deterministic microgrinding and under loose-abrasive lapping. Similarly, Fig. 97.45 indicates that larger abrasives lead to higher surface roughness. However, the dependence of grinding-induced surface residual force on abrasive size is not entirely obvious.

It is well known that grinding of brittle surfaces with loose or bound abrasives induces a state of residual compression on the ground surface. This phenomenon is often referred to as the Twyman effect.[7] The measured power (sag) of the surface is an indication of the extent of the residual force per unit of length along the edge of the ground surface. In the Twyman effect, a thin brittle disk is ground on one side, without altering the other side. As a result of grinding, the ground side is in a state of compressive stress and becomes convex, whereas the other side (on which the power is measured) is concave. The measured power Δh (sag of the thin plate) was converted to an equivalent force P_0 per unit length along the circumference of the ground edge, as described in Ref. 7:

$$P_0 = \frac{4E}{3(1-\nu)}\Delta h\left(\frac{t}{D}\right)^2, \qquad (1)$$

where E is the Young's modulus, ν the Poisson ratio, t the plate thickness, and D the plate diameter. The computed force P_0 is shown in Fig. 97.46 for deterministic microgrinding and in Fig. 97.52 for the loose-abrasive lapping experiments.

The results in Fig. 97.46 show that the surface grinding force does not necessarily diminish as the size of the abrasive gets smaller. Rather, for deterministic microgrinding, the intermediate abrasive (10 to 20 μm) gives the lowest surface grinding force. This result may be a consequence of the onset of ductile grinding, i.e., suppression of lateral cracking as the dominant material-removal mechanism in favor of plastic scratching. Ductile grinding is known to lead to high surface grinding forces.[8]

The correlation, reported in Fig. 97.46, between grinding-induced surface force P_0 and indentation crack size $2c$ was first reported for optical glasses by Lambropoulos *et al.*,[7] whose results show that the same correlation holds also for glass-ceramics.

Figure 97.47 shows the lapping material removal rate versus the combination of mechanical properties, which was used previously by Lambropoulos *et al.*[9] in optical glasses, extending the work by Buijs and Korpel-Van Houten.[10,11] Thus, it is concluded that, in lapping of glass-ceramics,

$$\frac{dh}{dt} \sim \frac{E^{5/4}}{K_c H^2}, \tag{2}$$

where E is Young's modulus, K_c is fracture toughness, and H is the hardness. This correlation results from using a lateral crack model as the basis for the material removal mechanism.

Figure 97.48 shows the dependence of the surface roughness of the 22-μm alumina-lapped surface on the glass-ceramic hardness. As in optical glasses,[8]

$$\text{surface roughness} \sim \frac{1}{\sqrt{H}}. \tag{3}$$

The results for polishing material removal rate show that increasing hardness generally leads to a diminishing removal rate, an expected result (see Fig. 97.50). Figure 97.51 shows a new result, however, instances of which have been reported by Lambropoulos *et al.*[12,13] for polishing of optical glasses: The polishing rate has the same dependence on material properties combination $E^{5/4}/K_c$ Hv as the lapping rate (Fig. 97.47). This result is not unexpected from a fundamental point of view: since in any material removal process atomic bonds must be broken among surface atoms, a property characterizing such bond strength (for example, fracture toughness) is expected to influence the polishing removal rate.

Our measurements on the deterministic microgrinding and lapping of glass-ceramics also allow us to compare these two processes in terms of the material removal rate and quality (surface roughness, residual stresses) of the resulting surface. Table 97.III summarizes the data for the samples studied in this report. Deterministic microgrinding maintains a faster removal rate than lapping (over the range of lapping pressures and relative speeds used), while for comparable abrasive sizes the surface roughness is lower than that for lapping, and the grinding-induced surface residual forces are significantly reduced as compared to lapping.

Table 97.III: Comparison of deterministic microgrinding and loose-abrasive grinding (lapping) for the cold working of glass-ceramic materials (L is the nominal abrasive size used). For deterministic microgrinding the abrasives are diamonds embedded in a metal bond. For lapping and polishing the abrasives are alumina.

	Surface Removal Rate (μm/min)	rms Surface Roughness (μm)	Surface Residual Force (N/m)
Deterministic microgrinding (fixed infeed)			
$L = 70$ μm	100	1.2–1.7	400–1100
$L = 15$ μm	50	0.5–1	200–700
$L = 2$ to 4 μm	10	0.05–0.3	300–800
Lapping (fixed pressure)			
$L = 22$ μm	5–9	0.9–1	900–1300
$L = 7$ μm	1–4	0.7–0.8	800–1200
Polishing (fixed pressure)			
$L = 1$ μm	0.04–0.1	0.01–0.1	—

In this article mechanical and chemical properties of glass-ceramics and their response under deterministic or loose abrasive grinding conditions have been correlated. The quality of the resulting surface in terms of the material removal rate, the surface microroughness, and the surface residual stresses induced by microgrinding have been characterized. Neither the effects of material grain size and abrasive grain size nor the correlation of "feeds and speeds" have been examined since these alter the rate at which the tool penetrates into the work surface. In addition, the issue of subsurface damage and that of the deepest flaw induced by microgrinding have not been addressed. These issues should be studied in the context of the mechanical strength of the glass-ceramic components, especially in relation to applied thermal or mechanical forces acting on these components after grinding.

Conclusions

The microgrinding and polishing behavior of five novel glass-ceramics have been studied. The mechanical properties of the glass-ceramics, as well as their material removal rate and quality of the resulting surface, have been measured for deterministic microgrinding (fixed infeed rate; metal bond diamond cup wheel on a CNC machining platform; embedded diamond abrasives of 70 mm, 15 μm, and 3 μm in size), loose-abrasive lapping (fixed nominal pressure, 22 μm and 7 μm Al_2O_3 loose abrasives), and polishing (fixed nominal pressure, 1 μm Al_2O_3 abrasives). The quality of the worked surface was characterized in terms of the grinding-induced surface microroughness and the grinding-induced surface residual force.

Findings on deterministic microgrinding of glass-ceramics under fixed infeed rate include the following:

1. Workpiece surface microroughness scales linearly with chemical susceptibility of the glass-ceramics under alkali attack conditions. Higher mass loss under alkali attack generally leads to higher surface roughness in deterministic microgrinding and higher tool-wear rate.
2. Smaller bound abrasives lead to lower surface microroughness.
3. Intermediate bound abrasives (10 to 20 μm) lead to the lowest grinding-induced surface residual compressive force. Very large or very small bound abrasives lead to higher surface residual forces.
4. The grinding-induced surface residual compressive force increases with indentation-produced surface cracks; thus, microindentation may be used to predict surface-grinding force.

Findings on the loose-abrasive grinding and polishing of glass-ceramics under fixed nominal pressure include the following:

1. The lapping removal rate increases with $E^{5/4}/K_c$ Hv, as in optical glasses.
2. The surface roughness for 22-μm abrasives increases with $1/\sqrt{H}$, as in optical glasses.
3. The surface roughness for 22-μm abrasives increases with chemical susceptibility to alkali attack, as it did for deterministic microgrinding.
4. The polishing removal rate decreases with increasing hardness H, and increases with increasing $E^{5/4}/K_c$ Hv. This result identifies fundamental similarities between the lapping and polishing material removal mechanisms.
5. The grinding-induced surface residual compressive force is an increasing function of indentation-produced surface cracks; thus, microindentation may be used to predict surface-grinding force.

In comparing deterministic microgrinding with loose-abrasive microgrinding, it was found that deterministic microgrinding maintains a faster removal rate than lapping, while for comparable abrasive sizes, the surface roughness induced by deterministic microgrinding is lower than that for lapping, while the grinding-induced surface residual forces are significantly reduced.

REFERENCES

1. A. R. Boccaccini, J. Mater. Sci. Lett. **15**, 1119 (1996).

2. A. G. Evans, in *Fracture Mechanics Applied to Brittle Materials*, edited by S. W. Freiman (American Society for Testing and Materials, Philadelphia, 1979), Vol. ASTM STP 678, Part 2, pp. 112–135.

3. C. B. Ponton and R. D. Rawlings, Mater. Sci. Technol. **5**, 865 (1989).

4. *ibid.*, Mater. Sci. Technol. **5**, 961 (1989).

5. J. C. Lambropoulos, T. Fang, P. D. Funkenbusch, S. D. Jacobs, M. J. Cumbo, and D. Golini, Appl. Opt. **35**, 4448 (1996).

6. H. M. Pollicove and D. T. Moore, in *Optical Fabrication and Testing Workshop*, Vol. 24, 1992 Technical Digest Series (Optical Society of America, Washington, DC, 1992), pp. 44–47.

7. J. C. Lambropoulos, S. Xu, T. Fang, and D. Golini, Appl. Opt. **35**, 5704 (1996).

8. D. Golini and S. D. Jacobs, Appl. Opt. **30**, 2761 (1991).

9. J. C. Lambropoulos, S. Xu, and T. Fang, Appl. Opt. **36**, 1501 (1997).

10. M. Buijs and K. Korpel-van Houten, J. Mater. Sci. **28**, 3014 (1993).

11. *ibid*., Wear **166**, 237 (1993).

12. J. C. Lambropoulos, in *Optical Fabrication and Testing Workshop*, Vol. 7, 1996 OSA Technical Digest Series (Optical Society of America, Washington, DC, 1996), pp. 88–91.

13. J. C. Lambropoulos, S. D. Jacobs, and J. Ruckman, in *Finishing of Advanced Ceramics and Glasses*, edited by R. Sabia, V. A. Greenhut, and C. G. Pantano, Ceramic Transactions, Vol. 102 (The American Ceramic Society, Westerville, OH, 1999), pp. 113–128.